

Received 30 July 2024; accepted 15 August 2024. Date of publication 21 August 2024; date of current version 16 September 2024.  
The review of this article was arranged by Editor C.-M. Zetterling.

Digital Object Identifier 10.1109/JEDS.2024.3447022

# Temperature-Dependent Electrical Characteristics and Low-Frequency Noise Analysis of AlGaN/GaN HEMTs

QIANG CHEN<sup>1</sup>, Y. Q. CHEN<sup>2</sup> (Senior Member, IEEE), CHANG LIU<sup>2</sup>, ZHIYUAN HE<sup>2</sup>, YUAN CHEN<sup>2</sup>,  
K. W. GENG<sup>1</sup>, Y. J. HE<sup>2</sup>, AND W. Y. CHEN<sup>1</sup>

<sup>1</sup> School of Electronic and Information Engineering, South China University of Technology, Guangzhou 510641, Guangdong, China  
<sup>2</sup> Science and Technology on Reliability Physics and Application of Electronic Component Laboratory, China Electronic Product Reliability and Environmental Testing Research Institute, Guangzhou 511370, Guangdong, China

CORRESPONDING AUTHORS: C. LIU, Y. Q. CHEN, AND K. W. GENG (e-mail: xd\_liuchang@163.com; yiqiang-chen@hotmail.com; gengkw@scut.edu.cn)

This work was supported in part by the National Natural Science Foundation of China under Grant 62274043, and in part by the Key-Area Research and Development Program of Guangdong Province under Grant 2022B0701180002.

**ABSTRACT** In this paper, we investigate the electrical characteristics of AlGaN/GaN HEMTs at the lowest temperature of 20 K. The measurement results indicate that the output current of the device decreases significantly with increasing temperature at temperature ranging from 40 K to 260 K, and the saturation drain current decreases by 19%. The gate leakage current rises slightly when the temperature increases. However, both the transfer and C-V characteristics indicate that the threshold voltage shift slightly in a negative direction as the temperature rises. In order to determine the physical mechanism of electrical characteristics change, the low-frequency noise (LFN) characteristics at different temperatures were measured and the density of traps was extracted. Finally, we consider that there are two competing mechanisms affecting the electrical characteristics of devices. The trap density reduction caused by temperature rise leads to threshold voltage's negative shift, while the drop of 2DEG mobility is the main reason for the decrease of output current.

**INDEX TERMS** Low temperature, AlGaN/GaN HEMTs, LFN, traps.

## I. INTRODUCTION

AlGaN/GaN HEMTs have a wide range of applications in RF and high power fields due to their excellent material properties [1], [2], [3]. With the development of the aerospace industry, AlGaN/GaN HEMT with excellent characteristics has become an important candidate for the key components of spacecraft power systems, communication systems and radar systems. However, the extreme temperature variation and extremely low temperature in the space environment will put forward higher requirements for the reliability of devices. As results, it is very important to study low temperature reliability of AlGaN/GaN HEMTs and it is of great significance to investigate the electrical characteristics and carrier transport mechanism of devices at different ambient temperatures to realize the aerospace application. There have been several studies on the electrical characteristics and mechanism of GaN HEMT devices from low temperature

(~100 K) to high temperature (~400 K). Zhao et al. [4] investigated electrical characteristics of GaN devices at temperature ranging from 223 K to 398 K. They also concluded that the Schottky barrier height, series resistances and gate leakage current are very susceptible to temperature. Kim et al. [5] carried out research on AlInN/GaN HEMTs' electrical characteristics in the temperature range of (210 K, 420 K). They concluded that saturation drain current and maximum transconductance of the devices hardly changes with temperature. Zhang et al. [6] have studied physical mechanisms of reverse-bias leakage current in Al<sub>0.25</sub>Ga<sub>0.75</sub>N/GaN Schottky diodes in the temperature range of 110K to 400K. Cuerdo et al. [7] studied the characteristics of RF GaN devices in the process of going from 300 K to 100 K. They found that the transconductance, drain current and cut-off frequency increased with the decrease of temperature, which they attributed to the decrease of

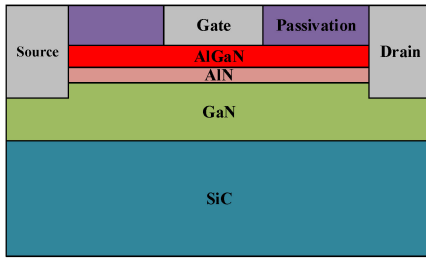


FIGURE 1. The schematic of cross section of DUTs.

optical phonon scattering at low temperature. But to date, the effects of temperature on the electrical characteristics of AlGaN/GaN HEMT in ultra-low temperature ( $\sim 40$  K) have been rarely reported.

The electrical characteristics of AlGaN/GaN HEMT are investigated with the temperatures at the lowest temperature of 20 K in this paper. The C-V and LFN tests are also carried out to analyze the physical mechanism of raps in the devices at different temperatures.

## II. EXPERIMENTAL DETAILS

The device structure used for the experiment shown in Fig. 1. Compared to traditional HEMT devices, this device has an AlN spacer layer between the AlGaN barrier layer and the GaN buffer layer. The thickness of barrier layer is 18 nm, the thickness of spacer layer is 1 nm and the thickness of buffer layer is  $2 \mu\text{m}$ . The substrate is silicon carbide. The gate Schottky contact metal electrode and the source-drain ohmic contact electrode are composed of Mo/Ti/Au (30/40/300 nm) and Ti/Al/Ni/Au (20/30/50/100 nm), respectively. The gate width of the device is 1.5 mm, and the gate length is  $0.5 \mu\text{m}$ . The space between gate and source is  $2 \mu\text{m}$  and the space between gate and drain is  $5 \mu\text{m}$ .

The I-V and C-V characteristics were measured by semiconductor device analyzer (Keithley 4200) and the LNA is measured by Low-Frequency Noise Analyzer (Keysight E4727A). All I-V and C-V measurement are carried out on the Lakeshore cryogenic vacuum probe station. In order to ensure the extremely low temperature environment, the devices must be sealed in a small test chamber and vacuum treatment is required.

## III. RESULTS AND DISCUSSIONS

### A. DC CHARACTERISTICS AT DIFFERENT TEMPERATURES

Fig. 2(a) is the output characteristics ( $I_{ds}$ - $V_{ds}$ ) of the device at different temperatures with  $V_{gs} = 0$  V and  $V_{ds}$  ranging from 0 V to 10 V. From Fig. 2(a), it is evident that the output current  $I_{ds}$  of the device decreases as the temperature increases. The drain current under the condition of  $V_{ds} = 10$  V and  $V_{gs} = 0$  V is defined as saturation drain current  $I_{ds,max}$ , which is extracted and plotted with temperature as the abscissa, as shown in Fig. 2(b). From Fig. 2(b), It can be seen that the variation of  $I_{ds,max}$  with temperature is approximately linear.  $I_{ds,max}$  decreases by 170.8 mA from 870.4 to 699.6 mA when the temperature rise from 40 K to 280 K.

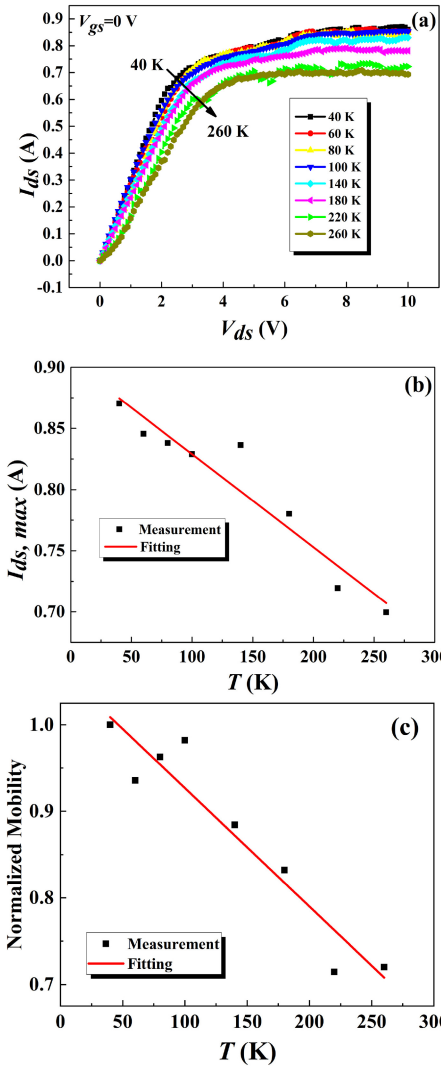


FIGURE 2. (a) Output characteristics, (b) saturated drain current and (c) normalized mobility at different temperatures.

In the saturation region, the equation of  $I_{ds,max}$  is [8]:

$$I_{ds,max} = \frac{\mu C_{ox} W}{2L} (V_{gs} - V_{th})^2 \quad (1)$$

where  $C_{ox}$  is the AlGaN unit barrier capacitance. Using the formula, the mobility at different temperatures can be derived. The normalized mobility curve with temperature is shown in Fig. 2(c). It can be found that the carrier mobility decreases by 19% with increasing temperature, which is consistent with [9]. This phenomenon indicates that phonon scattering play a key role at higher temperature among all scattering mechanisms, which is reported by earlier research [10], [11].

The transfer characteristics ( $I_{ds}$ - $V_{gs}$ ) are shown in Fig. 3(a) with  $V_{ds} = 5$  V. Consistent with the output characteristics,  $I_{ds}$  decreases with increasing temperature. The inset of Fig. 3(a) is the square law extrapolation of the transfer characteristics ( $I_{ds}^{1/2}$ - $V_{gs}$ ), which is used to obtain the threshold voltage  $V_{th}$  [5]. The relationship between  $V_{th}$  and temperature is shown in Fig. 3(b). Apparently,  $V_{th}$  has

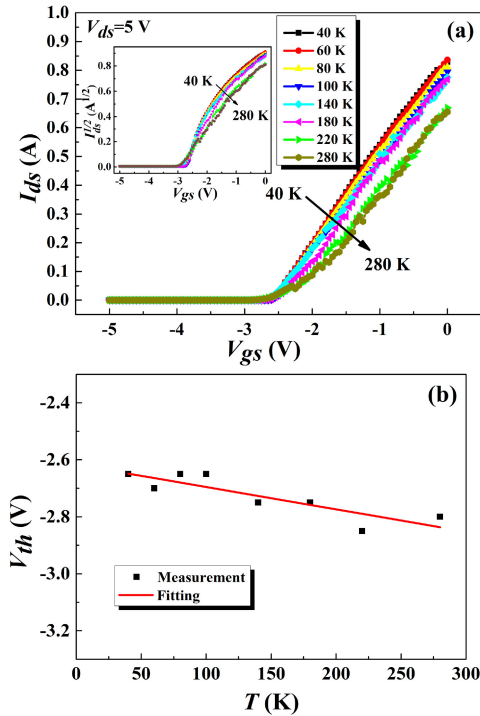


**FIGURE 3.** (a) Transfer characteristics and (b) threshold voltage  $V_{th}$  of AlGaN/ GaN HEMTs at different temperatures.

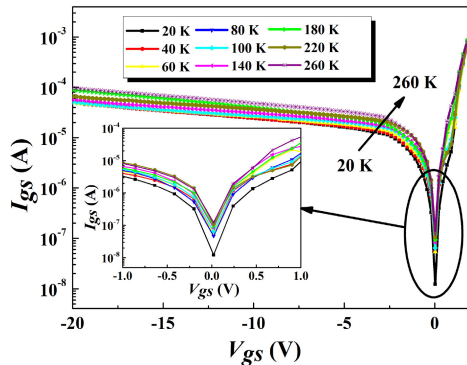


**FIGURE 4.** The gate-to-source characteristics of AlGaN/GaN HEMTs at different temperatures.

a slight negative shift about  $-0.15$  V with the increasing temperature. It is generally considered that the negative shift of  $V_{th}$  is related to the rise of 2DEG concentration. The more 2DEG concentration causes the device to require more negative gate voltage to reach full depletion, resulting in negative shift of  $V_{th}$ . However, the shift of  $V_{th}$  is very small, indicating that the increase of 2DEG concentration is not large. The mechanism of 2DEG concentration increase will be further analyzed in combination with low-frequency noise measurement.

Gate leakage current at different temperature was also measured as shown in Fig. 4. In order to show more clearly the temperature dependence of gate leakage, the inset amplifies the curve of  $I_{gs}$  under the condition of  $V_{gs}$  from

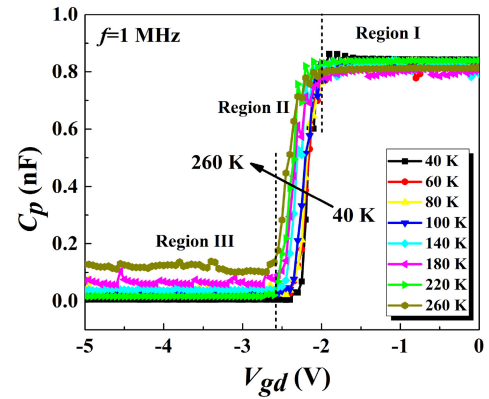


**FIGURE 5.** The C-V characteristics of AlGaN/GaN HEMTs at various temperature.

$-1$  V to  $1$  V. It is obvious from the inset of Fig. 4 that  $I_{gs}$  increases with rising temperature. Considering that the device used in this paper has an AlN spacer layer, so its barrier height and width are larger than the conventional AlGaN/GaN HEMT, the thermionic emission mechanism and direct tunneling mechanism may not be the main leakage current mechanism, because it is difficult for electrons to obtain enough energy to cross the barrier or directly pass through the barrier. Therefore, we believe that the dominant mechanism of gate leakage current is FP trap assisted tunneling, which has a positive correlation with temperature. With the increase of temperature, trap assisted tunneling is intensified, and the gate leakage current increases [6].

### B. C-V CHARACTERISTICS OF THE ALGAN/GAN HEMTs AT DIFFERENT TEMPERATURES

Fig. 5 shows the C-V characteristics of the device at different temperature, which can be divided into three regions according to the depletion state. The 2DEG accumulation region, the 2DEG depletion region and GaN buffer layer electron deep depletion region are shown in Fig. 5 from right to left. The Region I indicates the accumulation of 2DEG at the interface when the gate voltage is changed from negative to positive. Region II is the depletion zone of 2DEG, which reflects the gradual depletion of electrons from the interface to the buffer layer. And it's obvious that the capacitance decreases with the reduction of gate voltage. The depletion of 2DEG in the channel and the further depletion of electrons in the GaN buffer layer are reflected in the Region III. From Region II in Fig. 5, It is clear that the curves shift negatively as the temperature increases, and the threshold voltage also appears to drift negatively with increasing temperature, which is consistent with Fig. 3. The shift of the C-V curve is related to the interface state of the insulating layer/AlGaN and AlGaN/GaN [12].

### C. EFFECT OF TEMPERATURE ON LOW-FREQUENCY NOISE

As an efficient and nondestructive analysis method, LFN measurement can extract the defect density inside the device,

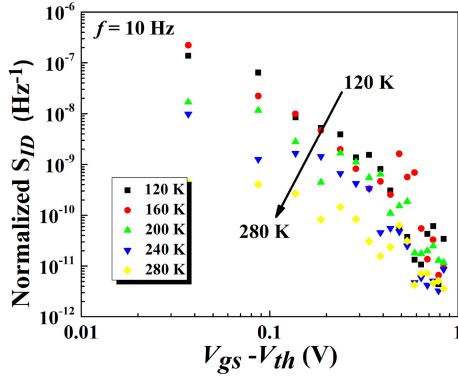


**FIGURE 6.** The typical  $S_{ID}/I^2$  at 10Hz versus  $V_{gs}-V_{th}$  at different temperatures.

and has been widely used in the field of GaN device failure analysis in recent years [13], [14], [15], [16]. In order to explore the temperature dependence of AlGaN/GaN HEMTs, the low frequency noise spectrum at different temperatures was obtained, and the drain current spectral noise density ( $S_{ID}$ ) was measured at  $V_{ds} = 0.1V$  as shown in Fig. 6.

There are two theories for low frequency noise, including the  $\Delta n$  theory and  $\Delta\mu$  theory. In  $\Delta n$  theory, the low frequency noise mainly comes from the fluctuation of carrier number, while in  $\Delta\mu$  theory, carrier mobility fluctuation is the main source of low frequency noise [17]. The carrier number fluctuation can be derived as (2). However, the  $\Delta n$ - $\Delta\mu$  model is now commonly used in GaN devices when the carrier number fluctuations induce noticeable changes in the mobility. In this model, the relationship of normalized drain current noise power spectrum density ( $S_{ID}$ ) and flat band voltage spectral density ( $S_{vfb,eff}$ ) is shown in (3) [18].

$$\frac{S_{ID}}{I_{ds}^2} = \frac{g_m^2}{I_{ds}^2} S_{vfb} \quad (2)$$

$$\frac{S_{ID}}{I_{ds}^2} = \left(1 \pm \alpha_c \mu_{eff} C_{ox} \frac{I_{ds}}{g_m}\right) \frac{g_m^2}{I_{ds}^2} S_{vfb} \quad (3)$$

The normalized  $S_{ID}/I_{ds}^2$  at 10 Hz is showed in Fig. 6 versus temperature.

Combining with (2) and (3), the  $S_{ID}/I_{ds}^2$  can be rewritten as follows:

$$\frac{S_{ID}}{I_{ds}^2} = \frac{g_m^2}{I_{ds}^2} S_{vfb,eff} \quad (4)$$

Afterwards, the effective trap density ( $N_{T,eff}$ ) can be obtained by using (5):

$$S_{vfb,eff} = q^2 k T \lambda N_{T,eff} / W L f C_{ox}^2 \quad (5)$$

where  $\lambda = 0.5$  nm is the AlGaN/GaN conduction band alignment [13]. According to (5), the  $S_{vfb,eff}$  and the extracted  $N_{T,eff}$  are shown in Fig. 7 at various temperatures. From Fig. 7, the effective trap density decreases with the increase of temperature. At lower temperatures, the trap density decreased rapidly, but with the increase of

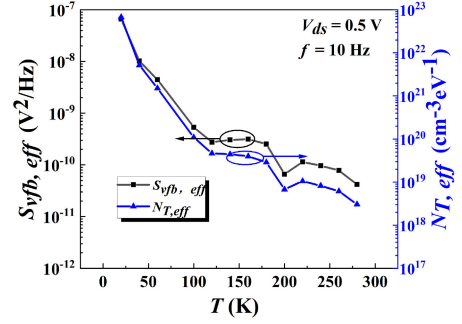


**FIGURE 7.** The extracted  $S_{vfb,eff}$  and  $N_{T,eff}$  at various temperatures from LFN measurement.

temperature, the decrease rate gradually became smaller. This result explains the negative shift of the threshold voltage. The threshold voltage can be expressed by the following equation [19].

$$V_{th} = \phi - \Delta E_C - \frac{q N_d d_d^2}{2 \epsilon_0 \epsilon_r} - \frac{q \sigma}{\epsilon_0 \epsilon_r} (d_d + d_i) \quad (6)$$

where  $\phi$  is the Schottky barrier height,  $\sigma$  is the charge density. It can be seen from Fig. 4 that the positive gate leakage current curves at different temperatures are basically parallel, so the Schottky barrier height at different temperatures does not change much. Therefore, according to (6), the change of threshold voltage is mainly related to charge density. The decrease in the effective density of traps in Fig. 7 leads to an increase in 2DEG concentration, which induces negative shift of threshold voltage.

#### D. PHYSICAL MECHANISM OF TEMPERATURE-DEPENDENT ELECTRICAL CHARACTERISTICS

According to the LFN measurement, trap density of AlGaN/GaN HEMT decrease as the temperature increases, which leads to the increase of 2DEG concentration in the channel. As shown in Fig. 8, as the temperature rises, more and more captured electrons gain enough energy to be released from the trap, replenishing the 2DEG. This explains  $V_{th}$ 's negative shift. However, there is clearly another dominant factor in the decrease of output current  $I_{ds}$ . From Fig. 2(c), the mobility drops significantly during the process of temperature rise, which dominates the output current degradation. The degradation of carrier mobility may be attributed to acoustic phonon scattering [20], [21]. It is believed that the loss of hot electron energy mainly comes from phonons, and the electron mobility limited by phonons inversely proportional to temperature.

#### IV. CONCLUSION

In this paper, we investigate the electrical characteristics of AlGaN/GaN HEMTs at the lowest temperature of 20 K. By measuring the DC, C-V and low-frequency noise characteristics of the device at different temperatures, we find that  $I_{ds}$

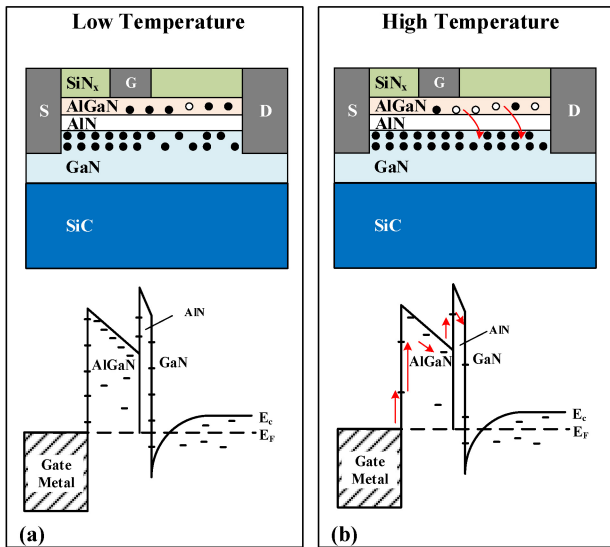


**FIGURE 8.** The mechanism of the AlGaN/GaN HEMTs at different temperature from LFN measurement. The filled circles represent occupied states, and the empty circle the unoccupied state.

decreases,  $V_{th}$  shifts negatively, and  $I_{gs}$  increases as the temperature increases. By the low frequency noise measurement, the extracted effective trap density of AlGaN/GaN HEMT decrease with the increasing temperature, which leads to the threshold voltage's negative shift. The degradation of  $I_{ds}$  can be mainly explained by the reduced carrier mobility.

## REFERENCES

- [1] O. Aktas, Z. F. Fan, S. N. Mohammad, A. E. Botchkarev, and H. Morkoc, "High temperature characteristics of AlGaN/GaN modulation doped field-effect transistors," *Appl. Phys. Lett.*, vol. 69, no. 25, pp. 3872–3874, Dec. 1996, doi: [10.1063/1.117133](https://doi.org/10.1063/1.117133).
- [2] S. C. Binari, K. Doverspike, G. Kelner, H. B. Dietrich, and A. E. Wickenden, "GaN FETs for microwave and high-temperature applications," *Solid State Electron.*, vol. 41, no. 2, pp. 177–180, Jan. 1997, doi: [10.1016/S0038-1101\(96\)00161-X](https://doi.org/10.1016/S0038-1101(96)00161-X).
- [3] C. Guo, Y. Ren, L. Gao, H. Zhu, and S. Li, "The investigation of AlGaN/GaN HEMT failure mechanisms under different temperature conditions," in *Proc. 2nd Int. Conf. Adv. Mech. Eng. Ind. Inform. (AMEII)*, 2016, pp. 995–1000, doi: [10.2991/ameii-16.2016.190](https://doi.org/10.2991/ameii-16.2016.190).
- [4] M. Zhao, X. Y. Liu, Y. K. Zheng, Y. Li, and S. Ouyang, "Analysis of the device characteristics of AlGaN/GaN HEMTs over a wide temperature range," *Mater. Sci. Eng. B*, vol. 178, no. 7, pp. 465–470, Apr. 2013, doi: [10.1016/j.mseb.2013.01.022](https://doi.org/10.1016/j.mseb.2013.01.022).
- [5] S. Kim, K.-S. Ahn, J.-H. Ryou, and H. Kim, "Temperature-dependent DC characteristics of AlInN/GaN high-electron-mobility transistors," *Electron. Mater.*, vol. 13, no. 4, pp. 302–306, Jul. 2017, doi: [10.1007/s13391-017-1606-1](https://doi.org/10.1007/s13391-017-1606-1).
- [6] H. Zhang, E. J. Miller, and E. T. Yu, "Analysis of leakage current mechanisms in Schottky contacts to GaN and  $\text{Al}_{0.25}\text{Ga}_{0.75}\text{N}/\text{GaN}$  grown by molecular-beam epitaxy," *J. Appl. Phys.*, vol. 99, no. 2, Jan. 2006, Art. no. 23703, doi: [10.1063/1.2159547](https://doi.org/10.1063/1.2159547).
- [7] R. Cuervo et al., "Temperature-dependent high-frequency performance of deep submicron AlGaN/GaN HEMTs," *Phys. Status Solidi*, vol. 5, no. 9, pp. 2994–2997, May 2008, doi: [10.1002/pssc.200779240](https://doi.org/10.1002/pssc.200779240).
- [8] S. M. Sze and K. K. Ng, *Physics of Semiconductor Devices*. Hoboken, NJ, USA: Wiley, 2006, doi: [10.1002/0470068329](https://doi.org/10.1002/0470068329).
- [9] R. Yahyazadeh and Z. Hashempour, "Effect of temperature on the electronic current of two dimensional quantum well in AlGaN/GaN high electron mobility transistors (HEMT)," in *Proc. 27th Int. Conf. Microelectron.*, 2010, pp. 189–193, doi: [10.1109/MIEL.2010.5490501](https://doi.org/10.1109/MIEL.2010.5490501).
- [10] L. Hsu and W. Walukiewicz, "Effect of polarization fields on transport properties in AlGaN/GaN heterostructure," *J. Appl. Phys.*, vol. 89, no. 3, pp. 1783–1789, Feb. 2001, doi: [10.1063/1.1339858](https://doi.org/10.1063/1.1339858).
- [11] M. S. Shur, B. Gelmont, and M. A. Khan, "High electron mobility in two-dimensional electrons gas in AlGaN/GaN heterostructures and in bulk GaN," *J. Electron. Mater.*, vol. 25, no. 5, pp. 777–785 May 1996, doi: [10.1007/BF02666636](https://doi.org/10.1007/BF02666636).
- [12] M. Miczek, C. Mizue, T. Hashizume, and B. Adamowicz, "Effects of interface states and temperature on the C-V behavior of metal/insulator AlGaN/GaN heterostructure capacitors," *J. Appl. Phys.*, vol. 103, no. 10, Jun. 2008, Art. no. 104510, doi: [10.1063/1.2924334](https://doi.org/10.1063/1.2924334).
- [13] M. Silvestri, M. J. Uren, N. Killat, D. Marcon, and M. Kuball, "Localization of off-stress-induced damage in AlGaN/GaN high electron mobility transistors by means of low frequency 1/f noise measurements," *Appl. Phys. Lett.*, vol. 103, no. 4, Jul. 2013, Art. no. 43506, doi: [10.1063/1.4816424](https://doi.org/10.1063/1.4816424).
- [14] Y. Q. Chen et al., "Effect of hydrogen on defects of AlGaN/GaN HEMTs characterized by low-frequency noise," *IEEE Trans. Electron Devices*, vol. 65, no. 4, pp. 1321–1326, Apr. 2018, doi: [10.1109/ted.2018.2803443](https://doi.org/10.1109/ted.2018.2803443).
- [15] S. Yue et al., "High-fluence proton-induced degradation on AlGaN/GaN high-electron-mobility transistors," *IEEE Trans. Nucl. Sci.*, vol. 67, no. 7, pp. 1339–1344, Jul. 2020, doi: [10.1109/tns.2020.2974916](https://doi.org/10.1109/tns.2020.2974916).
- [16] Q. Chen et al., "Degradation behavior and trap analysis based on low-frequency noise of AlGaN/GaN HEMTs subjected to radio frequency overdrive stress," *IEEE Trans. Electron Devices*, vol. 68, no. 1, pp. 66–71, Jan. 2021, doi: [10.1109/ted.2020.3040698](https://doi.org/10.1109/ted.2020.3040698).
- [17] D. Rigaud, M. Valenza, and J. Rhayem, "Low frequency noise in thin film transistors," *IEE Proc. Circuits Devices Syst.*, vol. 149, no. 1, pp. 75–82, Mar. 2002, doi: [10.1049/ip-cds:20020063](https://doi.org/10.1049/ip-cds:20020063).
- [18] G. Ghibaudo, O. Roux, C. Nguyen-Duc, F. Balestra, and J. Brini, "Improved analysis of low frequency noise in field-effect MOS transistors," *Phys. Status Solidi*, vol. 124, no. 2, pp. 571–581, Apr. 1991, doi: [10.1002/pssa.2211240225](https://doi.org/10.1002/pssa.2211240225).
- [19] A. Kranti, S. Haldar, and R. S. Gupta, "An accurate charge control model for spontaneous and piezoelectric polarization dependent two-dimensional electron gas sheet charge density of lattice-mismatched AlGaN/GaN HEMTs," *Solid State Electron.*, vol. 46, no. 5, pp. 621–630, May 2002, doi: [10.1016/S0038-1101\(01\)00332-X](https://doi.org/10.1016/S0038-1101(01)00332-X).
- [20] K. J. Lee et al., "Investigation of phonon emission processes in an AlGaN/GaN heterostructure at low temperatures," *Appl. Phys. Lett.*, vol. 78, no. 19, pp. 2893–2895, May 2001, doi: [10.1063/1.1367310](https://doi.org/10.1063/1.1367310).
- [21] M. Miyoshi et al., "Nanostructural characterization and two-dimensional electron-gas properties in high-mobility AlGaN/AlN/GaN heterostructures grown on epitaxial AlN/sapphire templates," *J. Appl. Phys.*, vol. 98, no. 6, Sep. 2005, Art. no. 63713, doi: [10.1063/1.2060946](https://doi.org/10.1063/1.2060946).